

## Precise Determination of the Unperturbed $^8\text{B}$ Neutrino Spectrum

T. Roger,<sup>1,2,\*</sup> J. Büscher,<sup>1</sup> B. Bastin,<sup>1,\*</sup> O. S. Kirsebom,<sup>3</sup> R. Raabe,<sup>1,2</sup> M. Alcorta,<sup>4,†</sup> J. Äystö,<sup>5</sup> M. J. G. Borge,<sup>4</sup> M. Carmona-Gallardo,<sup>4</sup> T. E. Cocolios,<sup>1,‡</sup> J. Cruz,<sup>6</sup> P. Dendooven,<sup>7</sup> L. M. Fraile,<sup>8</sup> H. O. U. Fynbo,<sup>3</sup> D. Galaviz,<sup>4,9</sup> L. R. Gasques,<sup>9</sup> G. S. Giri,<sup>7</sup> M. Huysse,<sup>1</sup> S. Hyldegaard,<sup>3</sup> K. Jungmann,<sup>7</sup> W. L. Kruithof,<sup>7</sup> M. Lantz,<sup>10</sup> A. Perea,<sup>4</sup> K. Riisager,<sup>3</sup> A. Saastamoinen,<sup>5</sup> B. Santra,<sup>7</sup> P. D. Shidling,<sup>7</sup> M. Sohani,<sup>7</sup> A. J. Sørensen,<sup>3</sup> O. Tengblad,<sup>4</sup> E. Traykov,<sup>1,7</sup> D. J. van der Hoek,<sup>7</sup> P. Van Duppen,<sup>1</sup> O. O. Versolato,<sup>7,8</sup> and H. W. Wilschut<sup>7</sup>

<sup>1</sup>*Instituut voor Kern- en Stralingsfysica, KU Leuven, Belgium*

<sup>2</sup>*Grand Accélérateur National d'Ions Lourds, Caen, France*

<sup>3</sup>*Department of Physics and Astronomy, Aarhus University, Denmark*

<sup>4</sup>*Instituto de Estructura de la Materia, IEM-CSIC, Madrid, Spain*

<sup>5</sup>*Department of Physics, University of Jyväskylä, Finland*

<sup>6</sup>*Departamento Física, FCT, Universidade Nova de Lisboa, Portugal*

<sup>7</sup>*Kernfysisch Versneller Instituut, University of Groningen, The Netherlands*

<sup>8</sup>*Grupo de Física Nuclear, Departamento FAMN, Universidad Complutense, Madrid, Spain*

<sup>9</sup>*Centro de Física Nuclear da Universidade de Lisboa, Portugal*

<sup>10</sup>*Fundamental Fysik, Chalmers Tekniska Högskola, Göteborg, Sweden*

(Received 5 December 2011; published 18 April 2012)

A measurement of the final state distribution of the  $^8\text{B}$   $\beta$  decay, obtained by implanting a  $^8\text{B}$  beam in a double-sided silicon strip detector, is reported here. The present spectrum is consistent with a recent independent precise measurement performed by our collaboration at the IGISOL facility, Jyväskylä [O. S. Kirsebom *et al.*, *Phys. Rev. C* **83**, 065802 (2011)]. It shows discrepancies with previously measured spectra, leading to differences in the derived neutrino spectrum. Thanks to a low detection threshold, the neutrino spectrum is for the first time directly extracted from the measured final state distribution, thus avoiding the uncertainties related to the extrapolation of  $R$ -matrix fits. Combined with the IGISOL data, this leads to an improvement of the overall errors and the extension of the neutrino spectrum at high energy. The new unperturbed neutrino spectrum represents a benchmark for future measurements of the solar neutrino flux as a function of energy.

DOI: 10.1103/PhysRevLett.108.162502

PACS numbers: 23.40.Bw, 26.65.+t, 27.20.+n

Since the solar neutrino problem was discovered in 1968 [1], several experiments have collected data in order to improve the resolution on the measurement of the flux of solar neutrinos [2]. The experiments confirmed the discrepancy, both in magnitude and in the energy dependence of the flux, with respect to the predictions of the standard solar model. This inconsistency was solved by introducing a finite mass to the neutrinos, opening a possibility for matter-enhanced flavor oscillations [3,4]. The latter have recently been confirmed in SNO [5], Borexino [6], and KamLAND [7].

Neutrino oscillations modify not only the total flux of solar neutrinos but also their energy distribution. Experiments capable of measuring this energy dependence of the flux, such as Super-Kamiokande [8] and the aforementioned SNO, are mostly sensitive to the high energy part of the spectrum. There the flux is dominated by neutrinos from the  $\beta^+$  decay of  $^8\text{B}$ , with a small contribution (about 3 orders of magnitude lower) by neutrinos produced in the  $^1\text{H} + ^3\text{He}$  reaction (“hep” neutrinos). The latter was calculated theoretically [9] and seems to be in good agreement with the observational upper limit [10]. The unperturbed  $^8\text{B}$  neutrino spectrum, however, is

still under discussion. It is usually deduced from the shape of the  $\beta$ -delayed  $\alpha$ -particle spectrum, which reflects the distribution of the low-lying  $2^+$  states of  $^8\text{Be}$ , as illustrated in Fig. 1. This final state distribution has been measured at Notre Dame by Ortiz *et al.* using a coincident measurement of the two  $\alpha$  particles [11]. It has later been refuted by Winter *et al.* at Argonne [12] and Bhattacharya, Adelberger, and Swanson in Seattle [13], who found spectra shifted by 50 keV, by using techniques of implantation in a silicon detector and a single  $\alpha$ -particle measurement,

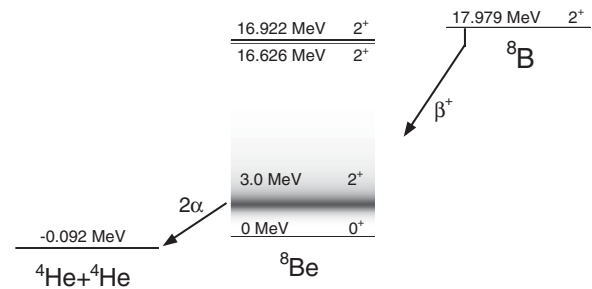


FIG. 1. Nuclear levels involved in the  $^8\text{B}$  decay chain. The  $\beta$  transition to the  $0^+$  ground state of  $^8\text{Be}$  is second forbidden and hence highly suppressed.

respectively. In Ref. [14], it was reported that the Notre Dame result suffered from underestimated uncertainties, dispelling the discussion. Recently, our collaboration has performed two new experiments. The first one at IGISOL (Jyväskylä, Finland), where the coincident  $\alpha$ -particle spectrum was measured after deposition of  $^8\text{B}$  nuclei on a thin carbon foil [15]. The maximum of the final state distribution was found to lie in between the Notre Dame prescription and the Argonne one, implying discrepancies at high neutrino energies. The second measurement, reported here, was designed to get a more reliable two- $\alpha$  final state distribution at low energies than in previous attempts, in order to significantly reduce the uncertainties on the upper-energy part of the neutrino spectrum. We used the technique of implantation in a finely segmented double-sided silicon strip detector (DSSSD) [16,17]. The  $^8\text{B}$  decays were identified through the time and position correlation between the implanted nuclei and subsequent decays. The two- $\alpha$  final state distribution at low energy was limited only by statistics, reaching down to 400 keV.

The measurement was performed at the Kernfysisch Versneller Instituut (KVI) at the University of Groningen, The Netherlands. The experimental arrangement is schematically shown in Fig. 2. A  $^8\text{B}$  beam was produced by fragmentation of a 55 MeV/u  $^{12}\text{C}$  beam on a 1.72 g/cm $^2$   $^{12}\text{C}$  target and analyzed with the TRI $\mu\text{P}$  magnetic separator [18], which was tuned to ensure the maximum transmission for  $^8\text{B}$  ions. An aluminum degrader with the appropriate thickness was placed before the detection setup to bring the beam energy down to 18.69(27) MeV before implantation in the DSSSD. The thickness of the implantation detector was 78  $\mu\text{m}$ , with an active area of  $16 \times 16$  mm $^2$ . Each side was divided in 48 strips oriented in perpendicular directions on the two faces. Coincident signals from the two sides identified one of the 2304 pixels of less than 0.1 mm $^2$  area. A 100  $\mu\text{m}$ -thick silicon diode ( $\Delta E$  in Fig. 2) was put in the beam path, upstream from the implantation detector, in order to identify the incoming ions via energy loss–time of flight correlations. The beam composition was  $^7\text{Be}$  (86.9%),  $^8\text{B}$  (6.3%),  $^9\text{C}$  (0.2%), and 6.6% of light stable ions. The  $^8\text{B}$  beam intensity was about

7 ions/s for a full cocktail beam intensity of 110 ions/s. Given the short half-life of  $^8\text{B}$  (770 ms), this implantation rate ensured the correlation between the implantation and the decay in the same pixel and, thus, the purity of the recorded  $^8\text{B}$  decay spectrum. Energy loss calculations performed by using the TRIM code [19] predicted an implantation depth of 26(5)  $\mu\text{m}$  for the  $^8\text{B}$  nuclei. Placed behind the DSSSD, a 300  $\mu\text{m}$ -thick silicon detector (Veto in Fig. 2) was used to tag the light particles (mainly protons) that could reach the detection setup.

The DSSSD was cooled down to 5  $^\circ\text{C}$  by using low odor base solvent, to improve both on the energy resolution, which reached 11 keV for the 5.48 MeV  $\alpha$  particles of  $^{241}\text{Am}$ , and on the stability of the detected signals, resulting in a gain variation of 3 keV at 3 MeV over a period of 5 days. The detection threshold of the electronic chain was measured with a pulser to be 200 keV in average (the details of the procedure are described in Ref. [17]). Specific attention was paid to the calibration procedure, to reduce the related uncertainties to a minimum. The implantation detector was calibrated by using  $^{148}\text{Gd}$ ,  $^{139}\text{Pu}$ ,  $^{241}\text{Am}$ , and  $^{244}\text{Cm}$  external  $\alpha$ -particle sources (with energies between 3 and 6 MeV). The  $\alpha$ -particle energy peaks were fitted by using a Gaussian function folded with two exponential tails as described in Ref. [20], accounting for the straggling taking place in the dead layer of the DSSSD. The thickness of this dead layer was first measured by using an external  $\alpha$  source with different incidence angles. The value reported in Ref. [17] is 340(3) nm. We have then remeasured this thickness, by using  $\beta$ -delayed  $\alpha$ -particle emission of implanted  $^{20}\text{Na}$  ions for the energy calibration. The three largest  $\alpha$ -particle emitting branches in  $^{20}\text{Na}$  decay provided calibration points at 2.691(1), 3.099(2), and 5.544(3) MeV [21]. The pulse height defect from the recoiling  $^{16}\text{O}$  ions was estimated to be between 48 and 57 keV for the different  $\beta$ -delayed  $\alpha$  branches by using the TRIM code in full cascade mode. With this calibration, the energy from  $\alpha$  particles emitted by an external source was measured and then compared with TRIM calculations. The average dead-layer thickness was found to be 336(7) nm. The combined measurements give a thickness of 339(3) nm, which translates into a 2 keV error on the calibration process.

The energy spectrum measured in the decay of the implanted  $^8\text{B}$  nuclei is determined by the final state energy distribution of the  $\beta$ -delayed  $\alpha$  particles, with an additional contribution due to the emitted  $\beta$  particles (“ $\beta$  summing”). The latter is small, as the  $\beta$  particles, statistically, deposit only a little amount of energy within one pixel. In addition, the measured spectrum is distorted by the  $\alpha$ -particle detection efficiency: Starting at energies beyond 3–4 MeV, a small fraction of the  $\alpha$  particles escapes from the pixel where the decay takes place, depositing only a part of the energy. The two effects,  $\beta$  summing and  $\alpha$  efficiency, generate a distortion function

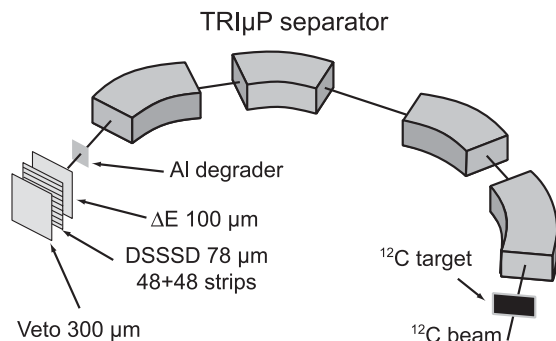


FIG. 2. Overview of the experimental setup used for the present experiment.

that, convolved with the original two- $\alpha$  final state distribution, produce the measured spectrum. The distortion function was determined by using a full simulation of the implantation and decay processes, realized with the GEANT4 package [22]. The position of the decay within the pixel was randomized according to the implantation profile; the direction of the emitted  $\alpha$  particles and leptons was randomized in three dimensions, taking into account angular correlations according to a pure Gamow-Teller transition, as the decay to the  $2_1^+$  state that dominates the spectrum is believed to be so [23]. Concerning the energy distribution of the decay ( $Q$  value), since the undistorted spectrum was initially not available, the measured spectrum was used instead. The ratio between the spectrum resulting from the convolution and the source spectrum provided a correction factor, which is shown in Fig. 3 as a function of the  $^8\text{Be}$  excitation energy  $E_x = E_{2\alpha} - 92$  keV. In a following step, the measured spectrum was divided by this factor to obtain a first approximation of the undistorted spectrum. The convergence of the deconvolution process was checked by using this first approximation to calculate a second-step correction factor (red line in Fig. 3). This is almost indistinguishable from the first one; the new convolved spectrum, calculated by using the first-approximation unperturbed spectrum as the source, differs from the measured one by less than the standard deviations in each bin, thus validating the procedure.

The correction factor drops down to about 0.2 at low energies. This is essentially due to the  $\beta$  summing, which shifts the measured spectrum by about 25 keV (as described in Ref. [17]), thus effectively removing events in this energy region. From about 3 MeV up, the correction factor is mainly determined by  $\alpha$  particles, which escape the detector when their energy is larger than about 10 MeV,

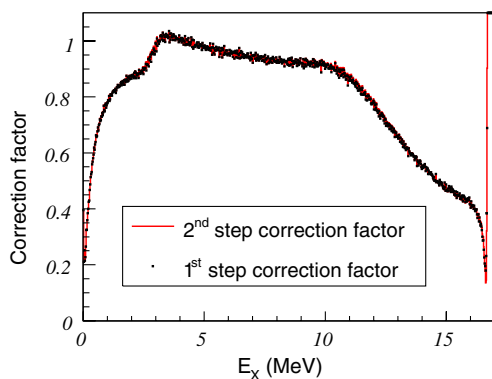


FIG. 3 (color online). Correction factor, accounting for the  $\beta$  summing and the  $\alpha$ -particle detection efficiency, applied to the measured final state distribution, as a function of the  $^8\text{Be}$  excitation energy  $E_x = E_{2\alpha} - 92$  keV. Black squares, first step correction generated by using the measured spectrum as the source; red line, second-step correction generated by using the corrected spectrum as the source.

appearing instead as events in excess in the region 3–10 MeV (as they deposit only part of their energy).

Note that the correction function is not normalized to unity. This reflects the fact that the number of events is not conserved by the convolution operation. In order to remain consistent, the ratio of the statistical errors to the number of counts for each bin was taken from the measured spectrum. The error on the energy scale associated with this process was estimated to be 2 keV, by varying the parameters of the simulation.

With the sole purpose of comparing the present results with previous ones, the deconvolved final state distribution was fitted by using the alternative  $R$ -matrix formalism described in Refs. [15,24,25], as presented in Fig. 4. This formalism allows us to easily fix the energy and reduced width of an arbitrary number of states. The fitting function was folded with the detector resolution. The result of the fit, where only the statistical errors were considered, gave an agreement of  $\chi^2/\nu = 1.21$ . The comparison with previous studies is shown in Fig. 5, together with the total error budget for the KVI and the IGISOL spectra.

The maximum of the present final state distribution is found at 2.925(6) MeV and appears to be shifted by +26, -14, and -18 keV with respect to the ones from Notre Dame [11], Argonne [12], and Seattle [13], respectively. The maximum of the IGISOL final state distribution was found at 2.921(5) MeV [15], hence strengthening the present result.

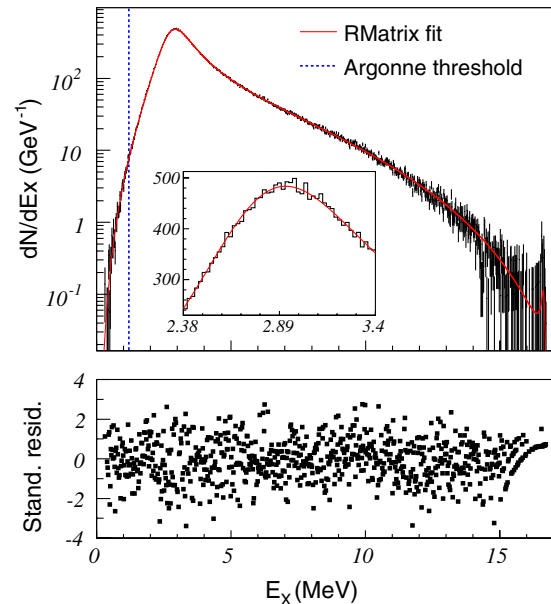


FIG. 4 (color online). Upper panel: Final state distribution of the  $2^+$  states in  $^8\text{Be}$  populated in the decay of  $^8\text{B}$ , as deduced in this Letter, and corresponding error bars. The curve is the result of an  $R$ -matrix fit. The inset shows a magnification in the peak region. The dotted blue vertical line indicates the detection threshold achieved in the Argonne experiment. Lower panel: Standardized residues of the fit.

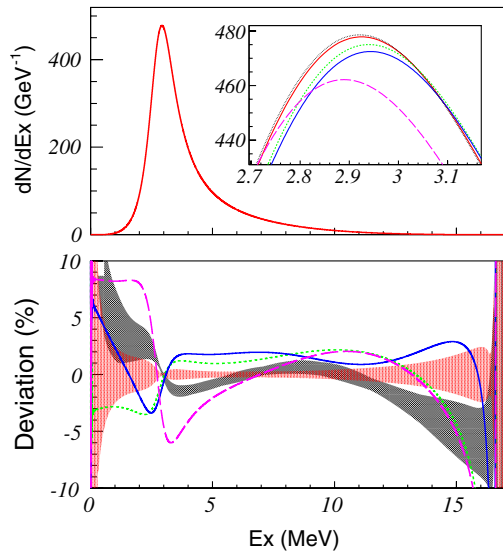


FIG. 5 (color online). Upper panel: Final state distribution deduced in this Letter. The inset is a zoom on the maximum of the distribution. Lower panel: Relative deviations from the previous studies at Notre Dame [11] (purple long-dashed curve), Argonne [12] (green short-dashed curve), Seattle [13] (blue dotted-dashed curve), and IGISOL [15] with its uncertainty (black shaded area). The KVI uncertainty is represented by the red shaded area.

Because of a low detection threshold and the absence of proton contamination, the present measurement of the  $\beta$ -delayed two- $\alpha$  spectrum was extended down to 400 keV. The  $^8\text{B}$  lepton spectra were consequently deduced directly from the measured final state distribution, thus avoiding the additional uncertainties introduced by the extrapolation of  $R$ -matrix fits below the detection threshold previously attained. The  $R$ -matrix formalism was used here only to propagate the errors to the lepton spectra. Following the procedure adopted by Winter *et al.*, both systematic uncertainties and statistical errors were propagated from the measured spectrum to the neutrino distribution through the  $R$ -matrix fit, by varying the values of the measured spectrum randomly within a  $1\sigma$  interval. The recoil order corrections were computed as prescribed in Ref. [26]. A detailed study of the influence of the new corrections proposed in Ref. [27] will be presented in a forthcoming article. The radiative corrections were taken from Ref. [28]. A consistent neutrino spectrum was extracted from the IGISOL  $R$ -matrix fit using the same corrections. The comparison between the KVI and the IGISOL neutrino spectra is shown in the upper panel of Fig. 6. A new spectrum was generated through an error-weighted average of the two spectra which agree at the level of a percent. All errors but the one on the recoil order term were taken into account in the procedure. The latter was added in quadrature to the result, leading to the error budget presented on the lower panel of Fig. 6. The comparison with the neutrino spectrum from Refs. [12,29] is also shown.

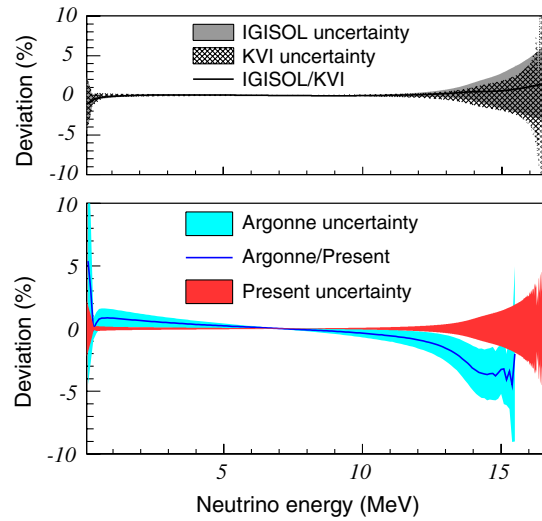


FIG. 6 (color online). Upper panel: Comparison between the KVI and the IGISOL neutrino spectra with their respective error budget. Lower panel: Uncertainty of the combined  $^8\text{B}$  neutrino spectrum deduced in the present study, compared with the one from Ref. [29].

The present spectrum shows non-negligible deviations from the Argonne spectrum in the range from 10 to 15 MeV. These deviations arise from the  $-14$  keV shift found in the  $\alpha$ -particle spectrum and will influence the interpretation of the solar neutrino spectrum shape. Possible reasons for this systematic shift have been investigated by our collaboration and are reported in Ref. [15] (Sec. IV.C Comparison to previous studies). The neutrino spectrum was extended to higher energies than previously attained and at the same time reduced the uncertainties. This is a consequence of the direct extraction of the neutrino spectrum from the measured final state distribution, suppressing the additional uncertainties due to the  $R$ -matrix model used in other works to complete the spectrum in regions where data were not available.

The deviations from the Argonne reference neutrino spectrum found here are smaller than the precision on the most recent solar neutrino fluxes reported [8]. However, they will influence the interpretation of the solar neutrino data in the next years, especially with an improvement in the solar neutrino statistics at energies above 14 MeV. The deviations have consequences on the upper limit on the solar hep neutrino signal and the diffuse supernova neutrino background [10], and the extension of the spectrum to higher neutrino energies leads to an improved determination of the  $^8\text{B}$  neutrino background that dominates direct detection experiments searching for dark matter particles [30].

This work was supported by FWO-Vlaanderen (Belgium), the IUAP-Belgian State Belgian Science Policy (BriX network P6/23), the Dutch FOM program 114 (TRI $\mu$ P), the European Union—Research Infrastructure Action under the FP6 “Structuring the

European Research Area” Program, and the Spanish projects FPA2009-07387, FPA2010-17142 and CSD2007-00042.

\*Present address: Grand Accélérateur National d’Ions Lourds, Caen, France.

†Present address: Physics Division, Argonne National Laboratory, Argonne, IL 60439, USA.

‡Present address: Physics Department, CERN, CH-1211 Geneva 23, Switzerland.

§Present address: Max-Planck-Institut für Kernphysik, Heidelberg, Germany.

- [1] R. Davis, D.S. Harmer, and K.C. Hoffman, *Phys. Rev. Lett.* **20**, 1205 (1968).
- [2] J. Bahcall and C. Peña-Garay, *New J. Phys.* **6**, 63 (2004).
- [3] L. Wolfenstein, *Phys. Rev. D* **17**, 2369 (1978).
- [4] S. P. Mikheyev and A. Y. Smirnov, *Sov. J. Nucl. Phys.* **42**, 913 (1985).
- [5] Q. R. Ahmad *et al.*, *Phys. Rev. Lett.* **89**, 011301 (2002).
- [6] G. Bellini *et al.* (Borexino Collaboration), *Phys. Rev. D* **82**, 033006 (2010).
- [7] S. Abe *et al.* (KamLAND Collaboration), *Phys. Rev. C* **84**, 035804 (2011).
- [8] S. Fukuda *et al.* (Super-Kamiokande Collaboration), *Phys. Rev. Lett.* **86**, 5651 (2001).
- [9] J. N. Bahcall, A. M. Serenelli, and S. Basu, *Astrophys. J. Suppl. Ser.* **165**, 400 (2006).
- [10] B. Aharmim *et al.* (SNO Collaboration), *Astrophys. J.* **653**, 1545 (2006).
- [11] C. E. Ortiz, A. García, R. A. Waltz, M. Bhattacharya, and A. K. Komives, *Phys. Rev. Lett.* **85**, 2909 (2000).
- [12] W. T. Winter, S. J. Freedman, K. E. Rehm, and J. P. Schiffer, *Phys. Rev. C* **73**, 025503 (2006).
- [13] M. Bhattacharya, E. G. Adelberger, and H. E. Swanson, *Phys. Rev. C* **73**, 055802 (2006).
- [14] E. G. Adelberger *et al.*, *Rev. Mod. Phys.* **83**, 195 (2011).
- [15] O. S. Kirsebom *et al.*, *Phys. Rev. C* **83**, 065802 (2011); **84**, 049902(E) (2011).
- [16] D. Smirnov *et al.*, *Nucl. Instrum. Methods Phys. Res., Sect. A* **547**, 480 (2005).
- [17] J. Büscher, J. Ponsaers, R. Raabe, M. Huysse, P. V. Duppen, F. Aksouh, D. Smirnov, H. Fynbo, S. Hyldegaard, and C. Diget, *Nucl. Instrum. Methods Phys. Res., Sect. B* **266**, 4652 (2008).
- [18] G. Berg *et al.*, *Nucl. Instrum. Methods Phys. Res., Sect. A* **560**, 169 (2006).
- [19] J. F. Ziegler, J. P. Biersack, and M. D. Ziegler, <http://www.srim.org>.
- [20] G. Bortels and P. Collaers, *Appl. Radiat. Isot.* **38**, 831 (1987).
- [21] F. Ajzenberg-Selove, *Nucl. Phys.* **A490**, 1 (1988).
- [22] S. Agostinelli *et al.*, *Nucl. Instrum. Methods Phys. Res., Sect. A* **506**, 250 (2003).
- [23] R. D. McKeown, G. T. Garvey, and C. A. Gagliardi, *Phys. Rev. C* **22**, 738 (1980).
- [24] C. R. Brune, *Phys. Rev. C* **66**, 044611 (2002).
- [25] S. Hyldegaard, Ph.D. thesis, Aarhus University, 2010, [http://phys.au.dk/fileadmin/site\\_files/publikationer/phd/Solveig\\_Hyldegaard.pdf](http://phys.au.dk/fileadmin/site_files/publikationer/phd/Solveig_Hyldegaard.pdf).
- [26] L. De Braekeleer, E. Adelberger, J. Gundlach, M. Kaplan, D. Markov, and A. Nathan, *Phys. Rev. C* **51**, 2778 (1995).
- [27] T. Sumikama *et al.*, *Phys. Rev. C* **83**, 065501 (2011).
- [28] I. S. Batkin and M. K. Sundaresan, *Phys. Rev. D* **52**, 5362 (1995).
- [29] W. T. Winter *et al.*, *Phys. Rev. Lett.* **91**, 252501 (2003).
- [30] Jocelyn Monroe and Peter Fisher, *Phys. Rev. D* **76**, 033007 (2007).